HHS Public Access

Author manuscript

Biochem Pharmacol. Author manuscript; available in PMC 2024 July 26.

Published in final edited form as:

Biochem Pharmacol. 2022 August ; 202: 115143. doi:10.1016/j.bcp.2022.115143.

Ciliogenesis mechanisms mediated by PAK2-ARL13B signaling in brain endothelial cells is responsible for vascular stability

Karthikeyan Thirugnanam[1,2,$], **Shubhangi Prabhudesai**[1,2,$], **Emma Van Why**[1], **Amy Pan**[4], **Ankan Gupta**[1,2], **Koji Foreman**[3], **Rahima Zennadi**[5], **Kevin R. Rarick**[6], **Surya M. Nauli**[7], **Sean P. Palecek**[3], **Ramani Ramchandran**[1,2,*]

[1]Department of Pediatrics, Developmental Vascular Biology Program, Medical College of Wisconsin, Children's Research Institute (CRI), Milwaukee, WI

[2]Division of Neonatology, Developmental Vascular Biology Program, Medical College of Wisconsin, Children's Research Institute (CRI), Milwaukee, WI

[3]Department of Chemical and Biological Engineering, University of Wisconsin-Madison, Madison, WI

[4]Division of Quantitative Health Sciences, Medical College of Wisconsin, CRI, Milwaukee, WI

[5]Department of Medicine, Duke University, Durham, NC

[6]Division of Critical Care, Medical College of Wisconsin, CRI, Milwaukee, WI

[7]Department of Pharmaceutical Sciences, Chapman University, Irvine, CA

Abstract

In the developing vasculature, cilia, microtubule-based organelles that project from the apical surface of endothelial cells (ECs), have been identified to function cell autonomously to promote vascular integrity and prevent hemorrhage. To date, the underlying mechanisms of endothelial cilia formation (ciliogenesis) are not fully understood. Understanding these mechanisms is likely to open new avenues for targeting EC-cilia to promote vascular stability. Here, we hypothesized that brain ECs ciliogenesis and the underlying mechanisms that control this process are critical for brain vascular stability. To investigate this hypothesis, we utilized multiple approaches

[*]**Corresponding Author**: Ramani Ramchandran, PhD, Department of Pediatrics, CRI Developmental Vascular Biology Program, Medical College of Wisconsin, Suite# C3420, 8701 Watertown Plank Road, P.O. Box 26509, Milwaukee, WI 53226, USA. rramchan@mcw.edu, **Fax:** 414-955-6325.

[$]Equal contribution

Author contributions

KT: Provided intellectual input, performed cell culture experiments, collected data, analyzed data, collated figures and wrote parts of the paper.

SP: Provided intellectual input, performed zebrafish experiments, collected data, analyzed data, collated figures and wrote parts of the paper.

EVW: Performed zebrafish experiments, collected and analyzed data.

AP: Analyzed data and performed statistical analysis on the data presented in the paper and wrote this section of the paper.

AG: Provided intellectual input, performed flow cytometry experiments, collected data, analyzed data and wrote parts of the paper.

KF: Performed hESC-BMEC experiment, collected data, analyzed data and wrote methods section.

RZ: Provided intellectual input and edited the paper.

KR: Performed cell culture experiments, collected data, analyzed data, provided intellectual input and edited the paper.

SMN: Provided intellectual input and edited the paper.

SPP: Provided intellectual input, guided hESC-BMEC studies and edited the paper.

RR: Provided intellectual input into the project design, concept, provided resources, analyzed and interpreted data, collated figures, wrote and edited the paper.

including developmental zebrafish model system and primary cell culture systems. In the *p21 activated kinase 2 (pak2a)* zebrafish vascular stability mutant [*redhead* (*rhd*)] that shows cerebral hemorrhage, we observed significant decrease in cilia-inducing protein ADP Ribosylation Factor Like GTPase 13B (Arl13b), and a 4-fold decrease in cilia numbers. Overexpressing *ARL13B-GFP* fusion mRNA rescues the cilia numbers (1-2-fold) in brain vessels, and the cerebral hemorrhage phenotype. Further, this phenotypic rescue occurs at a critical time in development (24 h post fertilization), prior to initiation of blood flow to the brain vessels. Extensive biochemical mechanistic studies in primary human brain microvascular ECs implicate ligands platelet-derived growth factor-BB (PDGF-BB), and vascular endothelial growth factor-A (VEGF-A) trigger PAK2-ARL13B ciliogenesis and signal through cell surface VEGFR-2 receptor. Thus, collectively, we have implicated a critical brain ECs ciliogenesis signal that converges on PAK2-ARL13B proteins to promote vascular stability.

Keywords

cilia; PDGF-BB; VEGF-A; vasculature; brain; vascular integrity

1. Introduction

Vascular stability is a critical feature of tissue homeostasis, and a breach in vascular stability has dire consequences [1]. In organs such as brain, an unstable vasculature is likely to spill blood constituents into the surrounding brain parenchyma, a process called hemorrhage. During embryonic development, hemorrhage leading to ventricular blood pooling is referred to as intraventricular hemorrhage [2], which affects brain development, and in worst case scenario, leads to preterm death. A weakened vessel wall can also cause vessel ballooning, a condition often referred to as aneurysms, which makes the vessel prone to rupture [3]. Thus, maintaining vascular stability or integrity of the embryonic brain vessels is important for the development of the organism.

Endothelial cells (ECs) that line the inner most layer of blood vessel wall and brain pericytes (PCs) that cover the ECs often work in concert to maintain embryonic vascular stability [4, 5]. Many studies have gone into understanding the EC-PC crosstalk mechanisms facilitating this stability [5]. In particular, a cellular microtubule-based organelle, called cilia, has recently been implicated in mural cell recruitment to facilitate vascular stability [6]. Further, we and others have implicated the importance of endothelial cilia in mediating vascular stability [7, 8]. Cilia are expressed on the apical surface of endothelial cells (ECs) and play a critical role in sensing blood flow in the lumen [9–13]. In addition to flow sensing, primary non-motile cilium regulates the directional migration and barrier integrity of ECs [14]. In zebrafish, mutants with defects in EC-cilia show relatively normal brain morphogenesis patterns but still display vascular integrity issues, such as intracranial hemorrhage [7, 8]. Cilia in zebrafish ECs have been suggested to regulate shear stress, notch activation, and *fox1b* expression, thereby recruiting vascular PCs to promote vascular stabilization [6]. In mice, intraflagellar transport cilia protein mutants (*Ift172* and *Ift122*) show cranial neural tube defects and bleeding [15, 16]. Further, ECs from *Ift88* mouse mutants that show polycystic kidney disease, have defects in ciliary function and altered vascular barrier

function as they are highly permeable to dextran [14]. Importantly, the brain vascular hemorrhage defect observed in ciliary zebrafish mutants can be rescued by overexpressing the defective ciliary protein in ECs, suggesting an EC-cilia cell autonomous function in maintaining vascular stability [7, 8]. Thus, collectively, the EC-cilia has a critical function in maintaining vascular stability and vascular barrier function [17].

Despite endothelial cilia's importance in maintaining vascular stability, the mechanisms of how EC-cilia are formed, a process called ciliogenesis, and its relation to brain vascular stability is not known. Understanding EC ciliogenesis and its associated role with promoting vascular stability is likely to open doors for development of novel intervention strategies that can target EC-cilia to maintain vascular stability and in turn promote vascular barrier function. We hypothesized that EC-ciliogenesis and the mechanisms underlying brain EC cilia formation are critical for promoting brain vascular stability. In this study, we investigated the EC-ciliogenesis hypothesis in a genetic vascular stability zebrafish mutant (*redhead, pak2a*) [18, 19], and the underlying mechanisms responsible for EC-ciliogenesis in human brain primary microvascular ECs. In vivo, we identified that *intracellular vascular stability protein*: p21 activated kinase 2 (Pak2a), and *ciliogenesis protein*: ADP Ribosylation Factor Like GTPase 13b (Arl13b) [20–22] is required for promoting brain EC-ciliogenesis and vascular stability. In vitro, we demonstrate that *ligands*: platelet-derived growth factor-BB (PDGF-BB) and vascular endothelial growth factor-A (VEGF-A), through *receptor*: vascular endothelial growth factor receptor 2 (VEGFR2), trigger PAK2-ARL13B ciliogenesis.

2. Materials and Methods

2.1 Reagents.

Antibodies for westerns used in this study include ARL13B (Proteintech Cat # 17711-I-AP), PAK2 (Cell signaling Cat # 2608), VEGFR2 (Cell signaling Cat # 2479), β-actin (Cell signaling Cat # 4970), α-tubulin (Abcam Cat # Ab15246), acetylated tubulin (Proteintech Cat # 66200-1-Ig), pVEGFR2 (Y1059) (Millipore, Cat # ABS553) and pVEGFR2 (Y1175) (Cell signaling Cat # 2478). Recombinant proteins used in this study include human PDGF-BB recombinant protein (Thermo fisher Cat # PHG0045), and human VEGF-A_{165} recombinant protein (Thermo fisher Cat # PHC9394). Silencing RNAs (siRNA's) used in this study include *PAK2* siRNA (Dharmacon-Horizon discovery Cat # J-003597-10-0005), and VEGFR2 siRNA (Dharmacon-Horizon discovery Cat # J-003148-09-0005). Secondary antibodies for western include anti-rabbit-HRP (Cell signaling Cat # 7074) and anti-mouse-HRP (Cell signaling Cat # 7076).

2.2 Animal studies.

For this study, the zebrafish experiments at the Medical College of Wisconsin were approved under the IACUC protocol #'s 320 titled, "Blood Vessel Development in Zebrafish". Zebrafish were fed and raised in a recirculating water tank system maintained at 28.5°C (Aquaneering System). Breeding pairs were set up at night and embryos were collected in the morning. One cell stage embryos were assumed to be zero hpf. The *rhd*^{mi149} mutant was

procured from Dr. Sarah Childs, University of Toronto. Transgenic lines used in this study were from our previous work [8].

2.3 RNA injection to rescue zebrafish *rhd* mutant or *pak2a* MO phenotypes (approaches 1 & 2).

Plasmids containing mouse *ARL13B-GFP wild type* and *R78Q mutant* cDNAs were kind gifts from Dr. Sudipto Roy, Singapore. Plasmids were linearized using *Sal*I restriction enzyme and RNA was synthesized using the SP6 mMessage mMachine transcription kit, Ambion™ (Invitrogen Cat # AM1340). 1 nL of 100 ng/mL RNA was injected into one cell stage embryos from clutches obtained by crossing heterozygous *rhd* mutant heterozygous fish pairs or co-injected with *pak2a* MO. Uninjected embryo or control MO-injected clutches served as controls for mutant and morphant experiments respectively. The percentage of bleeders (phenotype) in each clutch were quantified at 52 hpf.

2.4 Plasmid injection & heat shock experiment (approach 3).

Hsp70::ARL13B-GFP plasmid was a kind gift from Dr. Sudipto Roy, Singapore. 1 nL of 100 ng/mL of plasmid was injected into one cell stage embryos from clutches obtained by crossing *rhd* mutant mutant heterozygous fish pairs. Uninjected embryo clutches were used as controls. Both the plasmid injected and uninjected fish were heat shocked for 1.5 h at 37°C. Some clutches were heat shocked at 24 hpf and others were heat shocked at 30 hpf (Fig. 3a).

2.5 *pak2a* morphant studies.

1 nL of 2 ng/nL of *pak2a* MO (2 ng/embryo) (Pak2e5i6, 5'-CATGCAGTTATTCACCTGTGAAGCT- 3') [19] was injected into one cell stage embryos obtained by crossing *Tg(kdrl:mCherry)* and *Tg(beta-actin:ARL13B-GFP)* transgenic fish. Two ng of standard control morpholino (5′-CCTCTTACCTCAGTTACAATTTATA-3′) was injected into the control group of embryos. The number of cilia were quantified in the metencephalic artery (MtA) and middle cerebral vein (MceV) blood vessels in *pak2a* MO-injected and control MO-injected fish. To determine if injection of mouse *wild type ARL13B-GFP* RNA rescues the number of cilia in the *pak2a morphants*, 1 nL of 4 ng/nL of *pak2a* MO (4 ng/embryo) was co-injected with 1 nL of 100 ng/mL mouse *ARL13B-GFP wild type* RNA into clutches obtained by crossing *Tg(kdrl:mCherry)* and *Tg(beta-actin:ARL13B-GFP)* transgenic fish. Four ng/embryo of control MO or *pak2a* MO alone were injected into the embryo clutches.

2.6 Cell culture.

Primary human brain microvascular endothelial cells (HBMECs) (Cell Systems Corporation Cat # ACBRI 376), and primary human brain umbilical vein endothelial cells (HUVECs) (Glyco Tech Inc) were maintained at 37°C in 5% CO_2 incubator in endothelial cell complete medium (Promocell, Cat # C22010). Primary human brain choroid plexus endothelial cells (HCPECs) (ScienCell Cat # 1300) were maintained in endothelial cell medium (ScienCell Cat # 1001). All cell culture wells were seeded equally, and wells were randomized to

control versus experimental conditions with duplicates or triplicates per condition. All experiments were performed between passage 4-6.

The brain ECs were characterized for vascular marker expression using Fluorescence Activated Cell Sorting (FACS)-based method. Primary brain ECs (HBMECs & HCPECs) were cultured at <90% confluency, harvested with TrypLE Express (Thermo Fisher Scientific, Cat # 12604021), washed 2 times with FACS buffer (1× PBS with 5% FBS and 0.1% NaN_3) at 300 g for 5 mins and were subsequently stained for flow cytometry. During this process, cells were first incubated with antibodies for cell surface markers along with Live/Dead fixable yellow dead cell stain (Thermo Fisher, Cat # L34968) for 30 mins at 4°C. Following staining, cells were washed 3 times with FACS buffer, fixed and permeabilized using Cytofix/Cytoperm buffer (BD, Cat # 554722) and subsequently stained for intracellular proteins. BD perm wash buffer (Cat # 554723) was used for intracellular staining and washing. Primary antibodies were incubated for 45 mins and secondaries for 30 mins at 4°C. After the completion of staining, cells were resuspended in FACS buffer, and were subsequently run on a flow cytometer (BD LSRFortessa). Sample acquisition was done using BD FACSDiva software, and FlowJo software was used for data analysis. Following are the primary antibodies used for EC characterization: claudin-5 (Invitrogen, Cat # 352588), CD105 (Biolegend, Cat # 323218), Tie2 (BD Biosciences, Cat # 566716), CD31 (Biolegend, Cat # 303120), VE-cadherin (BD Biosciences, Cat # 560874), β-actin (Cell Signaling Technology Cat # 4970P). Donkey anti rabbit AF568 secondary antibody (Thermo Fisher Cat # A10042) was used to detect primary antibody-bound β-actin. Primary antibodies were diluted 1:50, and secondary antibodies were diluted 1:500.

Human embryonic stem cell (hESC) culture and differentiation to brain microvascular endothelial-like cells (BMECs) were performed as previously described [23]. H9 hESCs were maintained in E8 media on Matrigel-coated tissue culture treated polystyrene plates and passaged when they reached 60-70% confluency with 7-8 mins of Versene treatment. Differentiations were started from 60–70% confluent wells dissociated with 7 mins of Accutase treatment and reseeded at 35,000 cells/cm^2 onto Matrigel-coated tissue cultured treated polystyrene plates in E8 + 10 μM Y-27632 (Tocris, Cat # 1254), to promote stem cell survival. After 24 h, medium was aspirated and replaced with E8; medium was then changed daily for two days. To initiate differentiation, cells were treated with DMEM/F12 + 1x MEM Non-Essential Amino Acids + 0.5x GlutaMAX + 0.1 μM β-mercaptoethanol + 4 μM CHIR99021 for 23.5 h. Cells were then switched to DMEM/F12 + 1x MEM Non-Essential Amino Acids + 0.5x GlutaMAX + 0.1 μM β-mercaptoethanol + 1x B-27, with medium replaced daily for five days. Medium was then switched to HESFM + 1x B-27 + 10 μM retinoic acid + 20 ng/mL bFGF for 48 h before detachment with 30-45 mins of Accutase treatment. Cells were replated for downstream analysis at ~100,000 cells/cm^2 onto plates coated with a solution of 20 μg/mL fibronectin and 80 μg/mL collagen IV in HESFM + 1x B-27 + 10 μM retinoic acid + 20 ng/mL bFGF. 24 h later medium was switched to HESFM + 1x B-27. Imaging and protein collection was performed on day 10.

Testing of the H9s revealed a small paracentric inversion in the short arm of chromosome 11. This change was relatively small and given the confirmatory nature of the experiments

these cells were used for; the data has been retained. However, it is important to note that this mutation is present within all experiments regarding the hPSC-BMECs.

2.7 Primary Brain ECs Transfection.

HBMECs were seeded in 6 well culture dishes with coverslip approximately 24 h prior to transfection. Respective siRNA (*control, PAK2, VEGFR2*) were transfected using Lipofectamine 2000 reagent (Gibco, Cat # 11668019), and incubated for 48 h. Protein targets ARL13B, PAK2, VEGFR2, and loading control α-tubulin or β-actin proteins were assessed. In experiments where ARL13B-expression plasmids were included, 24 h post *PAK2* siRNA transfection, *ARL13B-GFP* plasmid construct was transfected. Briefly, 1.5 μg of plasmid DNA (*ARL13B-GFP* WT or *ARL13B-GFP mutant*) were mixed with 3 μL Lipofectamine2000, and the mixture was incubated at room temperature for 15 min, and overlayed onto the cells. The cells, DNA and transfection reagent were incubated for another 24 h at 37°C. Cells were washed twice with PBS, replaced with complete growth medium, and incubated at 37°C until further experimentation such as primary cilia immunostaining.

2.8 Western blot.

Proteins were isolated from HBMECs and zebrafish embryos using RIPA buffer (Sigma Cat # R2078) with complete mini EDTA-free protease inhibitor cocktail (Roche Cat # 11836170001) and PhosSTOP phosphatase inhibitor (Roche Cat # 4906845001). After isolation, total protein was quantified. Cell lysates were used for probing of the following proteins: ARL13B, PAK2, VEGFR2, α-tubulin and β-actin. Anti-rabbit HRP, and anti-mouse HRP were secondary antibodies used for chemiluminescence detection. Quantification was done using ImageJ software and plotted against the house keeping control protein (α-tubulin or β-actin). In this software, we used a rectangle box tool to map the house keeping protein band intensity. All other protein bands were measured using the same size rectangle box. Measurement values are provided as area covered in the box. The value provided by ImageJ is divided by 1, which is recommended by ImageJ, and is the inverse pixel value. Then, inverse pixel value for each target protein is divided by the respective house-keeping protein value for a given lane, and data plotted as average across biological replicate samples, which is represented in a graphical format using GraphPad software.

2.9 Primary cilia immunostaining.

HBMECs: Cells were grown to confluence in 6-well plates or on coverslips for cilia detection experiment. All the immunofluorescence experimentation was performed by seeding the cells on the same day with similar seeding density. Cells were not contact inhibited or synchronized for cell cycle condition but were probed in their native state. We present images of ECs containing cilia in similar confluence area on the plate. Cells were then washed with 1X PBS (Gibco Cat 10010023) thrice and then fixed with 4% paraformaldehyde (Electron Microscopy Sciences Cat # 15710) for 15 mins. Fixed cells were washed again with 1X PBS before permeabilization with 0.1% Triton X-100 (BioRad cat# 1610407). This was followed by blocking in 4% BSA in PBS and overnight incubation with primary antibodies of ARL13B (Proteintech Cat # 17711-1-AP) at a dilution of 1:500.

Cells were again washed with 1X PBS and incubated with Alexa fluor-488 anti-rabbit secondary antibody (Invitrogen Cat # A21206) (1:500 Dilution) or for 90 mins at room temperature and washed before mounting with DAPI. For HUVECs staining (Fig. 5d), primary antibody was acetylated tubulin and secondary antibody was Alexa fluor-594 goat anti-mouse IgG (H+L) (Invitrogen Cat # A11032). Cells were mounted with VECTAshield antifade mounting medium with DAPI (LifeSpan Biosciences Cat # LS-J1033-10) and finally imaged in Zeiss confocal microscope at a magnification of 63X.

hPSC-BMECs: On day 10, 24 well ibidi imaging plastic plates (Ibidi Cat # 82426) coated as described earlier were washed twice with cold Dulbecco's phosphate buffer solution (DPBS Cat # 14190144) and then fixed in 4% paraformaldehyde (diluted with DPBS from 16% stock solution with 0.1% Triton-X) for 15-20 mins at room temperature. Wells were washed twice with DPBS, then primary antibodies (Proteintech anti-Arl13B Cat # 17711-1-AP, Sigma-Aldrich anti-acetylated alpha tubulin Cat # T7451-100 μL) were applied at 1:1000 dilution in 1% bovine serum albumin in DPBS overnight at 4°C. Cells were washed twice and then goat IgG anti-rabbit 647 (Thermofisher Cat # A11001) and goat anti-mouse IgG anti-mouse 488 (Thermofisher Cat # A21244) were applied at 1:200 dilution from manufacturer provided solutions in 1% bovine serum albumin for 1 hour at room temperature or 4°C overnight. Cells were washed twice, treated with 2 μg/mL Hoechst 33342 in DPBS for 5-15 mins and then switched to DPBS before fluorescence imaging on a Nikon TI2 epifluorescent microscope at 60x magnification.

2.9.1 Cilia quantification (Supplement Video).

a) Zebrafish.: To quantify the number of cilia in zebrafish vessels, the BZ-X Analyzer software (Keyence) was used. The z-stack function on the Keyence scope was used to image cilia. An appropriate pitch was selected to capture (~40) continuous images along the z-axis. The full focus function was used that selects and combines only the areas at their sharpest focus to produce focused images that cover the entire depth of the zebrafish embryos. For z-stack capture, the first slice of the z-stack was chosen starting at the depth of focus (upper limit) at which the blood vessels MtA and MCeV first came into focus. The end position (lower limit) of the z-stack was chosen at the depth of focus where the vessels ended just before they went out of focus. Individual z-slices were evaluated for cilia counts to confirm that the cilia counted were from inside the blood vessels and not from focal planes above or below the vessels. These focused images were used for quantifications as described below. See video for z-stacks.

Number of cilia per length of vessels: In the tool bar, 'X-Y measure' tool was selected. Using a 'segment line' tool, a segment line was drawn from one end of the blood vessel to the other end. If the vessel was curved, multiple segments were drawn.

Number of cilia per projected surface area of vessels: In the tool bar, 'Area measure' tool was selected. Using a 'polygon' tool, a polygon was drawn enclosing the blood vessel. The software calculates the area inside the polygon.

To count the number of cilia in vessels in the MtA and MCeV: In the tool bar 'X-Y measure' tool was selected, followed by selection of the 'count' tool, which gave the number

of cilia. The cilia number for MtA and MCeV were divided by length of each respective vessel segment to calculate the number of cilia per length (μm) of vessel. This number was multiplied by 100 to give the number of cilia per 100 μm length of vessel. Similarly, cilia number in MtA and MCeV were divided by the total projected surface area of each respective vessel type to calculate the number of cilia per projected area of each vessel. This number was multiplied by 1000 to give the number of cilia per 1000 μm^2 of projected area of each vessel. The values generated from these calculations were plotted in *y*-axis for the respective samples.

b) Cell culture.: For cell culture experiments, the number of cilia and its length were assessed by number of nuclei to cilia using ACDC v0.93 cilia specific software [24] which runs on a MATLAB platform. The program is automated for detecting and counting nuclei and cilia in the respective field and provides the average length of cilia in that field. The quantification was done both manually and in automation to eliminate any false positive or true negative cilia and compared. In the automation cilia quantification software, a key feature was applied which requests user input for false positive cilia, which are then manually excluded from the dataset. The software output is an excel file, which includes the information of number of nuclei, number of cilia and average length of cilia. This information was graphed as shown in Figs. 6 and 7. In the quantification, each dot represents one random field in a slide and the experiment was done in triplicates. For example, five dots in Fig. 6 represents 5 random fields in three slides. And the number of nuclei presented in the respective Figure legends is the cumulative of all the fields.

2.10 Statistical analysis.

A t test or one-way analysis of variance (ANOVA) was used to examine the effects of various conditions on the outcomes. Proportion of bleeders were compared using one-sided two sample Z test or Fisher's exact test. $P<0.05$ was considered significant. Tukey's test or Bonferroni correction was used to adjust for multiple comparisons. For some analyses (Figs. 2d–e), data were log transformed to improve fit. The log differences between groups were back transformed to obtain the geometric mean of the ratio. All statistical analyses were performed using SAS version 9.4 (SAS Institute, Cary, North Carolina) software.

3. Results

3.1 Arl13b cilia expression in vivo restores vascular stability.

To test our hypothesis whether endothelial cilia are associated with brain vascular stability, we investigated levels of Arl13b cilia protein [25] in a vascular stability zebrafish *redhead* (*rhd*^{mi149}) *pak2a* [18] mutant embryos hereby referred to as *rhd* mutant. The *rhd* homozygous mutants exhibit an embryonic CNS hemorrhage phenotype caused by a mutation in *p21-activated kinase 2a (pak2a)* gene. Immunoblotting analysis revealed significant decrease ($P<0.05$) in Arl13b protein levels in *rhd* mutant bleeders compared to WT control (Figs. 1a–b). In heterozygous *rhd* intercrosses, incomplete penetrance of phenotype leads to ~10% of embryos developing hemorrhage as opposed to the expected Mendelian ratio of 25% for a fully penetrant recessive mutation. Thus, we performed complementary morpholino (MO)-oligonucleotide based knockdown approaches

with previously efficacy-confirmed *pak2a* Mos [19]. Injection of 1-4 ng *pak2a* MO in zebrafish embryos phenocopies the embryonic cerebral hemorrhage of *rhd* phenotype (Figs. 1c–c', red arrow) when compared to control MO-injected embryos (Figs. 1d–d'). To assess the effect of reduced Arl13b expression on cilia, we performed *pak2a* knockdown in a double transgenic zebrafish line *Tg(bactin: ARL13B-GFP; Tg(kdrl: mCherry)* where in cilia and the vasculature were observed in green and red colors respectively. Fluorescent microscopic analysis (Figs. 2a–c') at 52 h post fertilization (hpf) *pak2a* MO-injected embryo showed fewer (4-fold) cilia compared to 2 ng control MO injected group in the brain vessels [mid cerebral veins (MCeV) and met encephalic artery (MtA) (Fig. 2d–e). The number of embryos showing bleeder phenotypes (hemorrhages) were also greater in *pak2a* MO group compared to control MO group (Fig. 2f, $p<0.001$).

Because MtA and MCeV are arterial and venous vessel respectively, we investigated whether the different flow patterns in these vessels would affect ciliogenesis. The number of cilia per 100 μm vessel length (Fig. 2d), and per 1000 μm^2 vessel area (Fig. 2e) were measured and averaged. Details for this quantification are described in the materials and methods section. Both measurements yielded similar results. In MtA, the number of cilia per 100 μm vessel length in the control group is 7.7 times (geometric mean of the ratio was used – see stat section) higher than the *pak2a* MO group (P=0.00003), and 1.6 times higher than the *pak2a* MO + *arl13b* mRNA group. In MCeV, the number of cilia per 100 μm vessel length in the control group is 3.2 times higher than the *pak2a* MO group (P=0.0166), and 2.1 times higher than the *pak2a* MO + *arl13b* mRNA group. The analysis for cilia numbers per 1000 μm^2 vessel area resulted in slightly higher numbers compared to the analysis for cilia numbers per 100 μm vessel length. The trend of lower cilia number per 1000 μm^2 vessel area in *pak2a* MO group compared to control continued, and the *pak2a* MO + *arl13b* mRNA group showed more cilia number than *pak2a* MO group. Across the artery (MtA) and vein (MCeV), the expected number of cilia in venous vessel is higher than the artery vessel (P=0.03) in *pak2a* MO group. These data collectively suggest that arterial vessel cilia are more susceptible to *pak2a* loss than venous cilia. However, not all arterial and venous brain vessels are the same, and thus this interpretation cannot be generalized. Together, less Arl13b, a cilia-inducing protein expression correlates with fewer cilia in brain vessels of *rhd* mutants.

To assess the functional relevance of cilia Arl13b expression in the *rhd* hemorrhage phenotype, we performed three independent complementary approaches that have respective strengths. In the *first and second approaches*, capped *Arl13b*-mRNA were injected into *pak2a* morphant embryos or *rhd* mutant embryos respectively at 1-cell stage and assessed for cilia numbers and intracranial hemorrhage phenotype at 52 hours post fertilization (hpf) (Fig. 3a). In the second approach, we included a mutant (R78Q) *Arl13b-GFP mRNA* [22] as a comparison tool for WT *Arl13b-GFP* mRNA. The mutation R78Q is homologous to R79Q human mutation identified in a ciliopathy (Joubert syndrome) and is in the highly conserved GTPase domain (Fig. 3b), which abrogates GTP-binding ability of ARL13b [20, 26]. The first two approaches lacked a temporal component for assessing the consequence of Arl13b expression. Thus, in a *third approach* (Fig. 3a), we injected a heat shock plasmid expressing mouse *Arl13b-GFP WT* protein into embryos obtained from *rhd* het cross at the

1-cell stage and induced expression at 24 hpf (prior to brain circulation) or 30 hpf (post brain circulation). Rescue for hemorrhage phenotype was assessed at 52 hpf (Fig. 3a).

Injecting capped mouse *Arl13b-GFP* mRNA at 1-cell stage into *pak2a* MO partially rescued the cilia numbers (Figs. 2c–c', d–e) and hemorrhage phenotype (Fig. 2f) when compared to control MO embryos. Similarly, *Arl13b-GFP WT mRNA* but not *Arl13b-GFP Mutant (R78Q)* mRNA [22] when injected into *rhd* mutant rescued (nearly 2-fold, P=0.02) the hemorrhage phenotype (Fig. 3c). In the temporal heat shock approach, *Arl13b-GFP* expression at 24 hpf rescues *rhd* mutant embryo hemorrhage phenotype at 52 hpf but inducing the *Arl13b-GFP* expression at 30 hpf does not (Fig. 3d). Together, these data suggest that during assembly of brain vasculature, Arl13b-cilia expression prior to initiation of brain circulation is critical for functionally restoring vascular stability *in vivo*.

3.2 Brain microvascular ECs cilia characterization.

To assess whether Pak2-Arl13b-mediated cilia changes observed in zebrafish model can also occur in human brain microvascular endothelial cells (HBMECs), we purchased primary HBMECs from Cell Systems, Inc. We characterized these cells by performing FACS analysis for EC junctional vascular markers (claudin5 & VE-cadherin), cell surface molecules (endoglin (CD105) [27], CD31 and Tie2) in HBMECs, and compared them to brain choroid plexus ECs (HCPECs) (Cell Systems, Inc.), which line the Blood Cerebrospinal Fluid-Blood barrier (BCSF-B). In HBMECs, all the probed vascular markers were enriched compared to HCPECs (Fig. 4). We then immunostained for ARL13B cilia in HBMECs, HCPECs and HUVECs (ECs from large venous vessel) (Fig. 5). Interestingly, HBMECs occasionally showed 2-cilia (Fig. 5a, white box) in addition to cells with single cilium. In HCPECs (Fig. 5b, white box and arrow) and HUVECs (Fig. 5c, white box and arrow) grown under sparse conditions, only one cilium was observed. HUVECs grown in a more confluent condition where they display cobblestone morphology (Fig. 5d, arrows) showed 2-cilia. In addition, hESC-derived BMEC-like cells also occasionally showed 2-cilia (Fig. 5e, arrows). These observations confirm the observation in vivo wherein brain ECs from collateral vessels in mice have been reported to contain multiple cilia [28]. Taken together, these data suggests that ECs under different culturing conditions in vitro are capable of showing more than 1-cilium, similar to ECs *in vivo*.

3.3 Arl13b cilia expression in brain ECs in vitro also restores cilia numbers.

To investigate PAK2-ARL13B-mediated cilia changes in primary HBMECs, we knocked down human *PAK2* by siRNA (efficacy data: Figs. 7h–i) and assessed its effect on cilia length and numbers by performing immunofluorescent (IF) staining for cilia (ARL13B). Nucleus (DAPI) was also stained and (Figs. 6a–b) the cilia number and length were quantified as described in the materials and methods section. Cilia number quantification was performed using an automated cilia software [24] and was later confirmed by manual counting. Both sets of quantification data are shown (Fig. 6b–b') but only images used for manual quantification are included (Figs. 6a, c & d). For cilia length, quantification is shown using the cilia software. PAK2 knockdown brain ECs compared to control knockdown ECs showed decreases in the length (1-fold, P<0.001) and number (2-fold, P<0.001) of cilia (Figs. 6a–b). To assess ARL13B's effect on brain EC ciliogenesis, we

overexpressed the ARL13B-GFP WT (Fig. 6c) and ARL13B-GFP mutant (R78Q) (Fig. 6d) plasmid (used previously in vivo) in PAK2 knockdown brain ECs. Compared to PAK2 knockdown ECs, overexpression of *ARL13B-GFP WT* plasmid in the *PAK2* knockdown brain ECs, significantly increased the number (1-fold, P<0.001) and length (1-fold, P<0.001) of cilia while overexpression of *ARL13B-GFP mutant (R78Q)* plasmid did not (Fig. 6b). In *ARL13B-GFP R78Q* mutant-expressing control siRNA ECs, we observed a decrease in cilia length and number when compared to non-transfected control siRNA ECs (Fig. 6a–b). The R78Q mutation occurs in the highly conserved GTPase domain of ARL13B, which in turn abrogates the ability of ARL13B to bind GTP and prevents downstream effector binding and function [20, 26, 29]. Thus, the ability of the *ARL13B-R78Q mutant* to localize to cilia [22] and cause a decrease in cilia length and number argues for a dominant negative gain-of-function for this mutant protein. Taking both the in vivo and in vitro results together, we conclude that the PAK2-ARL13B ciliogenesis signal is important for vascular stability.

3.4 Endothelial ligands PDGF-BB and VEGF-A induce EC-cilia length

To investigate signals that feed into PAK2-ARL13B signaling for ciliogenesis, we focused on PDGF-BB and VEGF-A ligands, and the receptor for VEGF (VEGFR2). These molecules have been implicated before in vascular stability [30–33]. Further, treatment of zebrafish with a PDGFR- β inhibitor caused brain hemorrhage [34]. PDGF and VEGF crosstalk through VEGFR2 has been implicated in HUVECs [33]. Thus, collectively, we hypothesize that ligands PDGF-BB and VEGF-A could influence ciliogenesis on brain ECs to promote vascular stability through VEGFR2 on ECs.

Primary HBMECs were treated with PDGF-BB (10 ng/mL for 60 mins) and VEGF-A_{165} (20 ng/mL for 5 mins) and assessed for ARL13B and PAK2 protein levels using western blotting (Fig. 7a). Both the ligands induce the expression of ciliary protein ARL13B and vascular stability protein PAK2 (Figs. 7a–b), and PDGF-BB continues to induce the expression of these proteins at longer time points of 10, 30 and 60 mins (Figs. 7c–d). To assess the effect of ligands on cilia numbers and length, similar to the earlier experiment, IF was performed with ARL13B antibody (Fig. 7e) and quantified as described in the methods section. Interestingly, PDGF-BB and VEGF-A_{165} treatment did not show increase in cilia number (Fig. 7f) but showed increases in cilia length (Fig. 7g, PDGF-BB: P=0.0021, VEGF-A: P=0.0006). To investigate if PAK2 is upstream or parallel to ARL13B, similar to what we observed in vivo (Figs. 1 & 2), we investigated ARL13B protein levels in *PAK2* knockdown brain ECs post PDGF-BB or VEGF-A_{165} treatments by western blotting (Figs. 7h–i). Upon *PAK2* knockdown, both PAK2 and ARL13B protein levels are lower, and treatment with ligands (PDGF-BB nor VEGF-A_{165}) does not rescue either protein levels (Figs. 7h–i). These results suggest that both PDGF-BB and VEGF-A_{165} ligands can induce ciliogenesis in brain ECs through PAK2-ARL13B-mediated signals.

3.5 VEGFR2 receptor is critical for PDGF-BB and VEGF-A-mediated ciliogenesis in brain ECs

ARL13B is a well-established inducer of cilia length [22]. Our results thus far suggest a hypothesis that PDGF-BB and VEGF-A_{165} induces PAK2-ARL13B signals in brain ECs to promote ciliogenesis. The next question is how do these ligands induce the vascular

stability-ciliogenesis signal? The ligands PDGF-BB and VEGF-A_{165} have both been linked to VEGFR2 receptor signaling in ECs [33]. Thus, we investigated the contribution of VEGFR2 to the ligand-induced PAK2-ARL13B signaling in ECs. Brain ECs treated with PDGF-BB (10 ng/mL) for 60 mins showed more VEGFR2 protein in the total lysate (Figs. 8a–b) compared to 10 and 30 mins. Further, the PDGF-BB did not induce VEGFR2 phosphorylation at the Y1175 and Y1059 phosphorylation sites (Figs. 8c–d). However, VEGF-A_{165} (20 ng/mL for 5 min) treatment triggers robust phosphorylation of Y1175 and Y1059 residues in addition to induction of total VEGFR2 protein levels (Figs. 8c–d). Because we observed total VEGFR2 protein level changes in the ligand treated conditions, to investigate VEGFR2's contribution to ligand-induced PAK2-ARL13B signaling in brain ECs, we used the silencing RNA (siRNA) approach. We silenced *VEGFR2* with *VEGFR2* siRNA and treated the brain ECs with PDGF-BB (Figs. 8e–f) and VEGF-A_{165} (Figs. 8g–h) and investigated the PAK2 and ARL13B protein levels in total lysates. In *VEGFR2* silenced PDGF-BB (10, 30 or 60 mins) (Figs. 8e–f) PAK2 and ARL13B proteins did not show an increase. VEGF-A_{165} treated (5 mins) (Figs. 8g–h) brain ECs showed increases in both PAK2 and ARL13B protein levels but upon *VEGFR2* siRNA treatment, ~72% decrease for PAK2 and 61% decrease for ARL13B were observed when compared to VEGF-A_{165} alone treated brain ECs. Taken together with our cilia staining data where both PDGF-BB and VEGF-A_{165} increase cilia length (Fig. 7g), our biochemical analysis suggests that PDGF-BB and VEGF-A_{165} through VEGFR2 promotes PAK2-ARL13B-mediated ciliogenesis in brain ECs.

4. Discussion

Recent studies from our group and others have suggested a role for endothelial cilia in promoting stability of the brain vasculature [7, 8]. Whether ciliogenesis is important for vascular stability is not known. In this study, we show that endothelial ciliogenesis is important for establishing the stability of the brain vasculature. We also provide a novel mechanism by which brain ECs-ciliogenesis occurs, namely through the PAK2-ARL13B signaling axis. The salient features of this study include: (a) PAK2-ARL13B signaling is critical for brain ECs ciliogenesis and is needed at a specific time during brain vascular assembly process to promote vascular stability; (b) Ligands VEGF-A and PDGF-BB facilitate PAK2-ARL13B ciliogenesis signals in brain ECs through VEGFR2. These results collectively suggest an important role for endothelial ciliogenesis in mediating vascular stability in the developing brain vessels.

Using a *pak2a* redhead (*rhd*) zebrafish mutant, which shows cerebral hemorrhage [18], we investigated the association of ciliogenesis to brain vascular stability. Pak2a is ubiquitously expressed in ECs, and its higher expression levels in CNS is suggested to explain the selective cerebral hemorrhage phenotype observed in the global loss of *Pak2a* in zebrafish [18, 19]. We focused on ARL13b protein to study cilia formation because ARL13b signaling is implicated in ciliogenesis in mammalian cells and zebrafish [20, 22]. Overexpressing *Arl13b* mRNA and protein in mammalian cells and zebrafish causes bulging of the ciliary membrane. These bulges travel along the length of the primary cilium, and facilitates membrane extension, which is a unique mechanism by which Arl13b causes increases in the length of ciliary membrane [22, 25, 35]. When *Arl13b-GFP WT mRNA* was overexpressed

in *pak2a* knockdown embryos, the cilia number and cerebral hemorrhage phenotype was rescued (Fig. 2d–f). Conversely, *Arl13b mutant-GFP mRNA (R78Q)* when overexpressed in *pak2a* knockdown embryos failed to rescue the cilia number or hemorrhage phenotype. The R78Q mutation in ARL13B is reported in a human ciliopathic disorder called Joubert syndrome [26] and affects ARL13B's GTPase activity. Thus, our data in *pak2a mutant* and morphants suggests that ARL13B's GTPase activity is important for stabilizing the brain vasculature. However, ARL13B's GTPase activity is not critical for ciliary localization of ARL13B protein [22]. PAK2a's kinase activity has also been reported to be important for vascular integrity [18]. Thus, together, signaling effector proteins of PAK2 & ARL13B are critical for the vascular stability process.

In the *Arl13b-GFP WT mRNA* rescue experiments, the mRNAs were injected into 1-cell stage *rhd* embryos. Thus, the time point in embryonic development when Arl13b is needed to promote vascular stability was not known. We used a conditional heat shock strategy (37°C for 90 mins) to activate gene expression at specific time in development, a method widely used in zebrafish model system [36, 37]. Using the heat shock method, we observed that inducing the expression of *Arl13b mRNA* at 24 hpf, a time point when flow is not commenced in brain vessels, and brain ECs are assembling, the *rhd* hemorrhage phenotype is rescued (Fig. 3d). At 24 hpf, the first major head vessel, primordial midbrain channel begins to assemble, and the lumen formation has not occurred, which happens after 28 hpf [8]. Interestingly, inducing Arl13b expression at 30 hpf fails to rescue the *rhd* cerebral hemorrhage phenotype (Fig. 3d). Thus, Arl13b expression seems to be critical during brain vessel assembly process. However, how ciliogenesis at 24 hpf embryonic stage facilitates vascular stability later (52 hpf) remains unknown and is an active area of investigation. We hypothesize that a combination of intrinsic (EC-autonomous/cilia-mediated) and extrinsic (EC-pericyte recruitment) factors are partly responsible for facilitating vascular stability.

To investigate the upstream signaling pathway that triggers PAK2-ARL13B ciliogenesis signal in brain ECs, we examined the effect of two ligands known for their role in stabilizing both ECs and PCs, namely PDGF-BB and VEGF-A_{165} isoform [5]. PDGF-BB and VEGF-A both increase the levels of PAK2 and ARL13B proteins albeit at different times, and also increase the length of cilia in brain ECs (Fig. 7e and f) but not numbers. Further, knocking down *PAK2*, the main upstream regulator of ARL13B in brain ECs ciliogenesis signal decreased cilia length and numbers. Similar to in vivo results, overexpression of *WT Arl13b* plasmid on *PAK2* knockdown brain ECs in vitro rescues ciliogenesis whereas the mutant *R78Q Arl13b* plasmid did not (Fig. 6). Thus, PAK2-ARL13B mediated signals that influence brain EC ciliogenesis is a cell autonomous effect. Interestingly, the R78Q mutant known to be localized to cilia [22] seems to show some activity in brain ECs wherein overexpressing this mutant decreases cilia numbers and size. We interpret this data to suggest that R78Q mutation has gained dominant negative function perhaps by influencing WT ARL13b protein function.

In terms of receptor VEGFR2, knocking down *VEGFR2* in HBMECs results in loss of both PDGF-BB and VEGF-A induced PAK2-ARL13B signals. Thus, VEGFR2 is functionally implicated in this dual ligand signaling in brain ECs and is a key regulator of ciliogenesis. Further, the VEGFR2-dependent ciliogenesis pathway can be initiated

both by the canonical VEGF-A and non-canonical PDGF-BB ligands. Thus, VEGF-A or PDGF-BB ligation causing VEGFR2-dependent ciliogenesis pathway in brain ECs is plausible, but the nature of this pathway has yet to be determined and is a limitation of this study. Our current working model, which is largely based on our data here and from previous publication [33] suggests a crosstalk mechanism between PDGF-BB and VEGF-A ligands to mediate VEGFR-2 phosphorylation triggered induction of PAK2-ARL13B proteins to induce ciliogenesis in brain ECs. In this working model, PDGF-BB up regulates VEGFR-2 protein level to the cell surface through an unknown mechanism, perhaps triggering intracellular trafficking mechanisms [38]. Surface VEGFR2 is now available for VEGF-A binding and phosphorylation and subsequent signal transduction to PAK2-ARL13B-mediated ciliogenesis. Our experimental evidence suggests that PAK2 is upstream of ARL13B in ciliogenesis both *in vivo* (Fig. 1 a–b) and *in vitro* (Fig. 7 h–i). However, much work is needed here to determine whether VEGFR-2 phosphorylation sequentially activates PAK2 and ARL13B proteins or activates both proteins independently. The time frame in which ciliogenesis signals are triggered in brain ECs seems remarkably quick, and further experiments are necessary to evaluate the various possibilities associated with this rapid ciliogenesis mechanism in ECs. For example, within the time frame of 5 mins, VEGF-A induces a 20-30% increase in intracellular signal (PAK2-ARL13B), resulting in changes in cilia length (Fig. 7c–d). This rapid response is unlikely to occur from changes in protein synthesis alone. Post translational modification of some of the proteins in this pathway to influence their levels is a plausible hypothesis. For example, palmitoylation of ARL13B is necessary for its stability and role in cilia formation [39], and sumoylation of VEGFR2 in endothelial cells regulates its intracellular trafficking [40].

To confirm whether the biochemical signals translate to changes in cilia structure or morphology, we stained brain ECs with cilia marker ARL13B antibody. We noticed that most HBMECs possess a single cilium. Interestingly, a fraction of brain ECs show more than one cilium (Fig. 7e, zoomed panels), a novel observation not reported previously in the literature for primary brain ECs *in vitro*. ECs that line the collateral pial brain vessels in mice have been shown to contain multiple cilia [28], which confirms our observation *in vitro*. Further, HUVECs under confluent cobblestone morphology conditions also show 2-cilia, and hESC-derived BMEC-like cells also occasionally show 2 cilia. Thus, it is possible for ECs *in vitro* to contain more than 1-cilium and is dependent on cell culture conditions. Whether these cilia fall under the non-motile primary cilium or motile cilia category is not known. Additional detailed investigations are needed to determine the relevance of the 2-cilia finding in primary ECs.

Our study raises several important questions. For example, a) What is the source of the PDGF-BB and VEGF-A ligands in vivo to carry out EC-ciliogenesis? b) How is the VEGFR2 receptor signaling coordinated between the ligands PDGF-BB and VEGF-A to facilitate EC-ciliogenesis? Perhaps, the most pressing question is how does EC-cilia promote vascular stability? Answers to some of the questions will facilitate the process of applying these concepts into the clinic to offer better treatment options for pediatric hemorrhage conditions. At the bear minimum, the conceptual innovation that EC-ciliogenesis during early embryonic brain vascular assembly process is a key event that is functionally relevant to vascular stability later in development warrants further research.

In summary, we uncover a novel signaling axis (Pak2-Arl13b) *in vivo* that is responsible for ciliogenesis and vascular stability. *In vitro*, we demonstrate in primary brain ECs that a non-canonical signaling mechanism that includes PDGF-BB and VEGF-A ligands acting through VEGFR2 receptor is responsible for promoting PAK2-ARL13B ciliogenesis signals.

Supplementary Material

Refer to Web version on PubMed Central for supplementary material.

Acknowledgements

We thank the Department of Pediatrics at the Medical College of Wisconsin, Children's Research Institute at Children's Wisconsin for supporting the Developmental Vascular Biology program with programmatic funds that partly facilitated this research. KT, SP, AP, KF, AG, KR, RZ, SPP, SMN and RR are partly supported by R61HL154254. KT, SP, AG and RR are also supported partly by program development funds from Children's Research Institute. We thank Dr. Shahram Eisa-Beygi, Mr. Jeremy Larson, Ms. Morgan Martin who all contributed to the initial stages of this project. We also thank members of the Developmental vascular biology program for their insights and feedback on the project.

References

[1]. Obermeier B, Daneman R, Ransohoff RM, Development, maintenance and disruption of the blood-brain barrier, Nat Med 19(12) (2013) 1584–96. [PubMed: 24309662]

[2]. Ballabh P, Intraventricular hemorrhage in premature infants: mechanism of disease, Pediatr Res 67(1) (2010) 1–8. [PubMed: 19816235]

[3]. Lindgren AE, Koivisto T, Bjorkman J, von Und Zu Fraunberg M, Helin K, Jaaskelainen JE, Frosen J, Irregular Shape of Intracranial Aneurysm Indicates Rupture Risk Irrespective of Size in a Population-Based Cohort, Stroke 47(5) (2016) 1219–26. [PubMed: 27073241]

[4]. Stratman AN, Davis GE, Endothelial cell-pericyte interactions stimulate basement membrane matrix assembly: influence on vascular tube remodeling, maturation, and stabilization, Microsc Microanal 18(1) (2012) 68–80. [PubMed: 22166617]

[5]. Gaengel K, Genove G, Armulik A, Betsholtz C, Endothelial-mural cell signaling in vascular development and angiogenesis, Arterioscler Thromb Vasc Biol 29(5) (2009) 630–8. [PubMed: 19164813]

[6]. Chen X, Gays D, Milia C, Santoro MM, Cilia Control Vascular Mural Cell Recruitment in Vertebrates, Cell Rep 18(4) (2017) 1033–1047. [PubMed: 28122229]

[7]. Kallakuri S, Yu JA, Li J, Li Y, Weinstein BM, Nicoli S, Sun Z, Endothelial cilia are essential for developmental vascular integrity in zebrafish, J Am Soc Nephrol 26(4) (2015) 864–75. [PubMed: 25214579]

[8]. Eisa-Beygi S, Benslimane FM, El-Rass S, Prabhudesai S, Abdelrasoul MKA, Simpson PM, Yalcin HC, Burrows PE, Ramchandran R, Characterization of Endothelial Cilia Distribution During Cerebral-Vascular Development in Zebrafish (Danio rerio), Arterioscler Thromb Vasc Biol 38(12) (2018) 2806–2818. [PubMed: 30571172]

[9]. Ando J, Yamamoto K, Flow detection and calcium signalling in vascular endothelial cells, Cardiovasc Res 99(2) (2013) 260–8. [PubMed: 23572234]

[10]. Egorova AD, van der Heiden K, Poelmann RE, Hierck BP, Primary cilia as biomechanical sensors in regulating endothelial function, Differentiation 83(2) (2012) S56–61. [PubMed: 22169885]

[11]. Hierck BP, Van der Heiden K, Alkemade FE, Van de Pas S, Van Thienen JV, Groenendijk BC, Bax WH, Van der Laarse A, Deruiter MC, Horrevoets AJ, Poelmann RE, Primary cilia sensitize endothelial cells for fluid shear stress, Dev Dyn 237(3) (2008) 725–35. [PubMed: 18297727]

[12]. Luu VZ, Chowdhury B, Al-Omran M, Hess DA, Verma S, Role of endothelial primary cilia as fluid mechanosensors on vascular health, Atherosclerosis 275 (2018) 196–204. [PubMed: 29945035]

[13]. Goetz JG, Steed E, Ferreira RR, Roth S, Ramspacher C, Boselli F, Charvin G, Liebling M, Wyart C, Schwab Y, Vermot J, Endothelial cilia mediate low flow sensing during zebrafish vascular development, Cell Rep 6(5) (2014) 799–808. [PubMed: 24561257]

[14]. Jones TJ, Adapala RK, Geldenhuys WJ, Bursley C, AbouAlaiwi WA, Nauli SM, Thodeti CK, Primary cilia regulates the directional migration and barrier integrity of endothelial cells through the modulation of hsp27 dependent actin cytoskeletal organization, J Cell Physiol 227(1) (2012) 70–6. [PubMed: 21837772]

[15]. Cortellino S, Wang C, Wang B, Bassi MR, Caretti E, Champeval D, Calmont A, Jarnik M, Burch J, Zaret KS, Larue L, Bellacosa A, Defective ciliogenesis, embryonic lethality and severe impairment of the Sonic Hedgehog pathway caused by inactivation of the mouse complex A intraflagellar transport gene Ift122/Wdr10, partially overlapping with the DNA repair gene Med1/Mbd4, Dev Biol 325(1) (2009) 225–37. [PubMed: 19000668]

[16]. Gorivodsky M, Mukhopadhyay M, Wilsch-Braeuninger M, Phillips M, Teufel A, Kim C, Malik N, Huttner W, Westphal H, Intraflagellar transport protein 172 is essential for primary cilia formation and plays a vital role in patterning the mammalian brain, Dev Biol 325(1) (2009) 24–32. [PubMed: 18930042]

[17]. Ma N, Zhou J, Functions of Endothelial Cilia in the Regulation of Vascular Barriers, Front Cell Dev Biol 8 (2020) 626. [PubMed: 32733899]

[18]. Buchner DA, Su F, Yamaoka JS, Kamei M, Shavit JA, Barthel LK, McGee B, Amigo JD, Kim S, Hanosh AW, Jagadeeswaran P, Goldman D, Lawson ND, Raymond PA, Weinstein BM, Ginsburg D, Lyons SE, pak2a mutations cause cerebral hemorrhage in redhead zebrafish, Proc Natl Acad Sci U S A 104(35) (2007) 13996–4001. [PubMed: 17715297]

[19]. Liu J, Fraser SD, Faloon PW, Rollins EL, Vom Berg J, Starovic-Subota O, Laliberte AL, Chen JN, Serluca FC, Childs SJ, A betaPix Pak2a signaling pathway regulates cerebral vascular stability in zebrafish, Proc Natl Acad Sci U S A 104(35) (2007) 13990–5. [PubMed: 17573532]

[20]. Duldulao NA, Lee S, Sun Z, Cilia localization is essential for in vivo functions of the Joubert syndrome protein Arl13b/Scorpion, Development 136(23) (2009) 4033–42. [PubMed: 19906870]

[21]. Li Y, Wei Q, Zhang Y, Ling K, Hu J, The small GTPases ARL-13 and ARL-3 coordinate intraflagellar transport and ciliogenesis, J Cell Biol 189(6) (2010) 1039–51. [PubMed: 20530210]

[22]. Lu H, Toh MT, Narasimhan V, Thamilselvam SK, Choksi SP, Roy S, A function for the Joubert syndrome protein Arl13b in ciliary membrane extension and ciliary length regulation, Dev Biol 397(2) (2015) 225–36. [PubMed: 25448689]

[23]. Qian T, Maguire SE, Canfield SG, Bao X, Olson WR, Shusta EV, Palecek SP, Directed differentiation of human pluripotent stem cells to blood-brain barrier endothelial cells, Sci Adv 3(11) (2017) e1701679. [PubMed: 29134197]

[24]. Lauring MC, Zhu T, Luo W, Wu W, Yu F, Toomre D, New software for automated cilia detection in cells (ACDC), Cilia 8 (2019) 1. [PubMed: 31388414]

[25]. Larkins CE, Aviles GD, East MP, Kahn RA, Caspary T, Arl13b regulates ciliogenesis and the dynamic localization of Shh signaling proteins, Mol Biol Cell 22(23) (2011) 4694–703. [PubMed: 21976698]

[26]. Cantagrel V, Silhavy JL, Bielas SL, Swistun D, Marsh SE, Bertrand JY, Audollent S, Attie-Bitach T, Holden KR, Dobyns WB, Traver D, Al-Gazali L, Ali BR, Lindner TH, Caspary T, Otto EA, Hildebrandt F, Glass IA, Logan CV, Johnson CA, Bennett C, Brancati F, G. International Joubert Syndrome Related Disorders Study, Valente EM, Woods CG, Gleeson JG, Mutations in the cilia gene ARL13B lead to the classical form of Joubert syndrome, Am J Hum Genet 83(2) (2008) 170–9. [PubMed: 18674751]

[27]. Fukumitsu R, Takagi Y, Yoshida K, Miyamoto S, Endoglin (CD105) is a more appropriate marker than CD31 for detecting microvessels in carotid artery plaques, Surg Neurol Int 4 (2013) 132. [PubMed: 24231754]

[28]. Zhang H, Chalothorn D, Faber JE, Collateral Vessels Have Unique Endothelial and Smooth Muscle Cell Phenotypes, Int J Mol Sci 20(15) (2019).

[29]. Miertzschke M, Koerner C, Spoerner M, Wittinghofer A, Structural insights into the small G-protein Arl13B and implications for Joubert syndrome, Biochem J 457(2) (2014) 301–11. [PubMed: 24168557]

[30]. Kemp SS, Aguera KN, Cha B, Davis GE, Defining Endothelial Cell-Derived Factors That Promote Pericyte Recruitment and Capillary Network Assembly, Arterioscler Thromb Vasc Biol 40(11) (2020) 2632–2648. [PubMed: 32814441]

[31]. Stiver SI, Tan X, Brown LF, Hedley-Whyte ET, Dvorak HF, VEGF-A angiogenesis induces a stable neovasculature in adult murine brain, J Neuropathol Exp Neurol 63(8) (2004) 841–55. [PubMed: 15330339]

[32]. Ball SG, Shuttleworth CA, Kielty CM, Vascular endothelial growth factor can signal through platelet-derived growth factor receptors, J Cell Biol 177(3) (2007) 489–500. [PubMed: 17470632]

[33]. Mamer SB, Chen S, Weddell JC, Palasz A, Wittenkeller A, Kumar M, Imoukhuede PI, Discovery of High-Affinity PDGF-VEGFR Interactions: Redefining RTK Dynamics, Sci Rep 7(1) (2017) 16439. [PubMed: 29180757]

[34]. Wang Y, Pan L, Moens CB, Appel B, Notch3 establishes brain vascular integrity by regulating pericyte number, Development 141(2) (2014) 307–17. [PubMed: 24306108]

[35]. Thorpe SD, Gambassi S, Thompson CL, Chandrakumar C, Santucci A, Knight MM, Reduced primary cilia length and altered Arl13b expression are associated with deregulated chondrocyte Hedgehog signaling in alkaptonuria, J Cell Physiol 232(9) (2017) 2407–2417. [PubMed: 28158906]

[36]. Murtha JM, Keller ET, Characterization of the heat shock response in mature zebrafish (Danio rerio), Exp Gerontol 38(6) (2003) 683–91. [PubMed: 12814804]

[37]. Shoji W, Sato-Maeda M, Application of heat shock promoter in transgenic zebrafish, Dev Growth Differ 50(6) (2008) 401–6. [PubMed: 18430027]

[38]. Silva JAF, Qi X, Grant MB, Boulton ME, Spatial and temporal VEGF receptor intracellular trafficking in microvascular and macrovascular endothelial cells, Sci Rep 11(1) (2021) 17400. [PubMed: 34462507]

[39]. Roy K, Jerman S, Jozsef L, McNamara T, Onyekaba G, Sun Z, Marin EP, Palmitoylation of the ciliary GTPase ARL13b is necessary for its stability and its role in cilia formation, J Biol Chem 292(43) (2017) 17703–17717. [PubMed: 28848045]

[40]. Zhou HJ, Xu Z, Wang Z, Zhang H, Zhuang ZW, Simons M, Min W, SUMOylation of VEGFR2 regulates its intracellular trafficking and pathological angiogenesis, Nat Commun 9(1) (2018) 3303. [PubMed: 30120232]

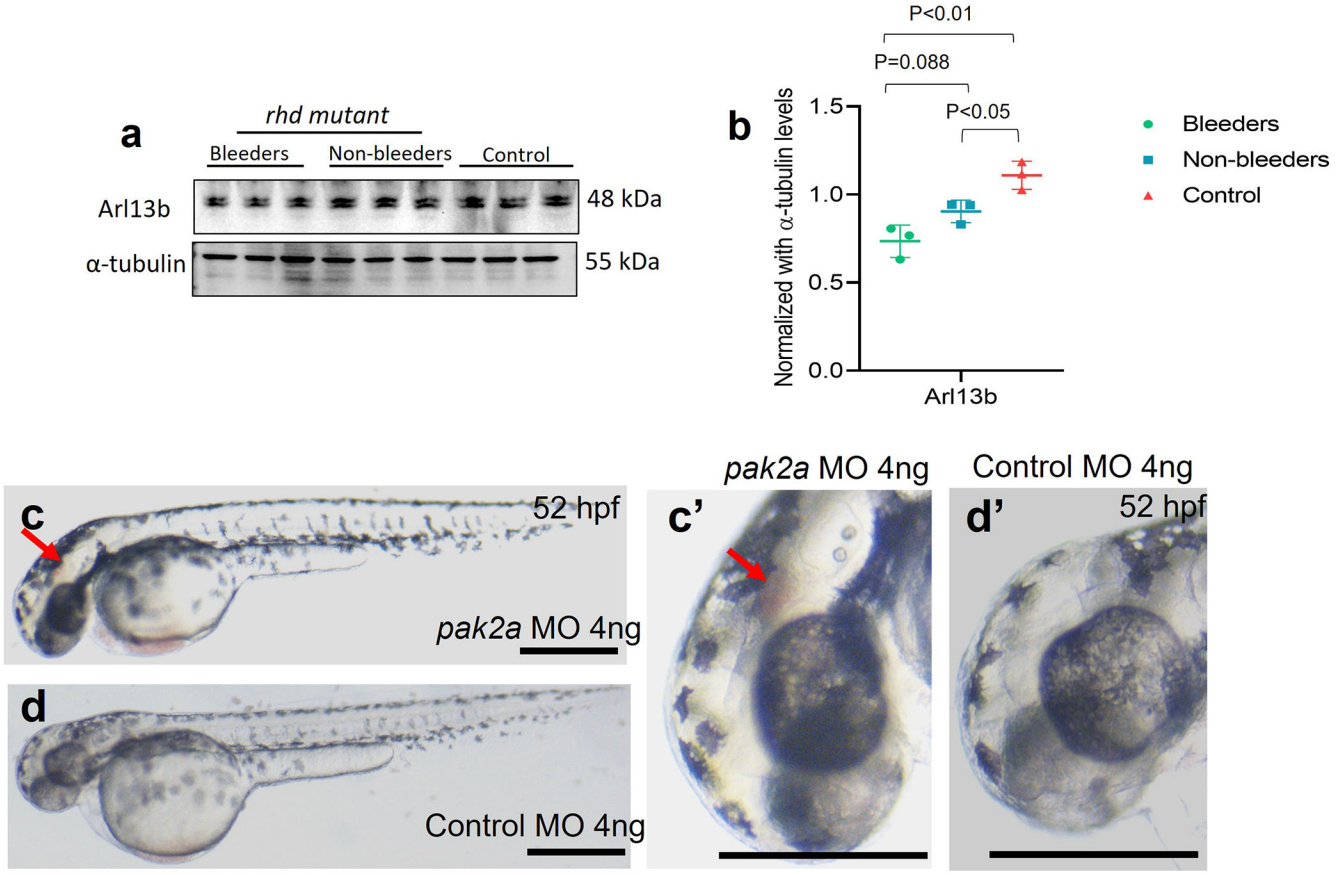

Figure 1. *pak2a* mutant or morphant fish show defective Arl13b cilia protein expression and cerebral hemorrhage phenotype.

a-b. Western blot of 52 hpf control or *rhd* mutant bleeder, non-bleeder embryo lysates and probed for Arl13b and a-tubulin proteins. Quantification of western blot in a is shown in panel b. *P<0.05; compared with control group; n=3 in each experimental group. Panels **c** & **d** are phase contrast images of 52 hpf embryos for *pak2a* MO and control MO respectively. Scale bars are 300 μm. Panels **c'** & **d'** are high power images of heads of 52 hpf embryos for *pak2a* MO and control MO respectively. Scale bars are 300 μm. Note: hemorrhage indicated by red arrow in *pak2a* MO. A t test was used to compare the experiment and control groups.

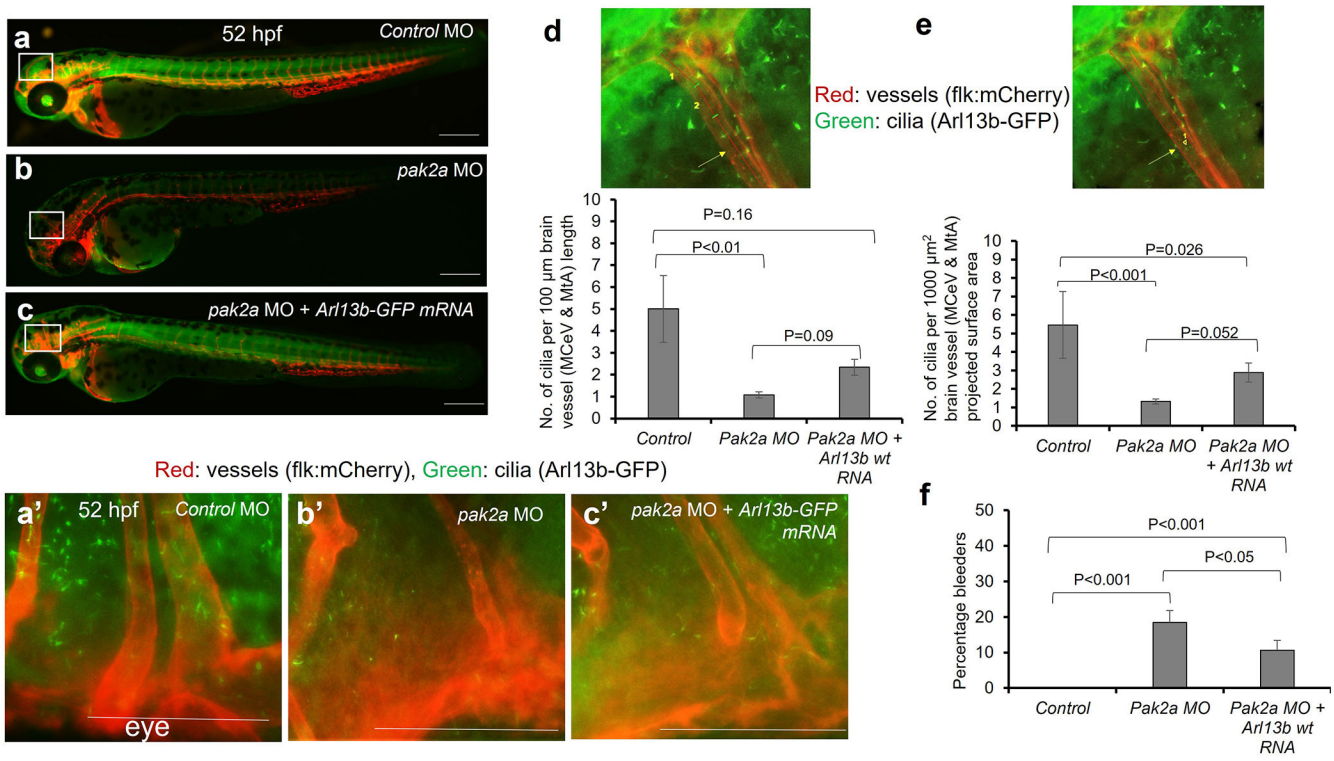

Figure 2. *pak2a* morphant fish show fewer cilia numbers and cerebral hemorrhage, which are partially rescued by arl13b WT mRNA.

a-b. Three groups of embryos are shown: control MO, *pak2a* MO and *pak2a* MO + *Arl13b-GFP* mRNA 52 hours post fertilization (hpf) fish. **a** and **a'** are control MO fluorescence images while **b** and **b'** are *pak2a* MO 52 hpf fluorescence images. **c** and **c'** are *pak2a* MO 52 hpf co-injected with *Arl13b-GFP* mRNA embryos. Scale bars for panels are 200 µm. Panels **a'-c'** are 100X images. Panels **d-f** are quantification for number of cilia in middle cerebral vein (MCeV) and metencephalic artery (MtA) blood vessels in the brain respectively from the 3 groups. The images on top of each panel show the quantification tool used for each image. **d** is number of cilia per 100 µm vessel length (note red line in image) while **e** is number of cilia per 1000 μm^2 projected surface area (note red box in image). For both panels **d** & **e**, red color denotes artery (MtA) panels and blue color represents vein (MCeV) panels. N= 5 embryos analyzed in each group were chosen randomly. Data was collated from 4 independent experiments. Results were plotted as mean ± SEM. P values less than 0.05 were considered significant. **f** depicts percent bleeders across the 3 groups. P values for the various group comparisons are indicated. Total number of surviving embryos for controls are 123, for *pak2a* MO are 118 and for *pak2a* MO + *Arl13b-GFP* are 123. One-way or two-way analysis of variance (ANOVA) was used to examine the effects of various conditions on the outcomes. Proportion of bleeders were compared using one-sided two sample Z test or Fisher's exact test. Quantification for panels **d** and **e** were performed on 40X images. See an example image in the video.

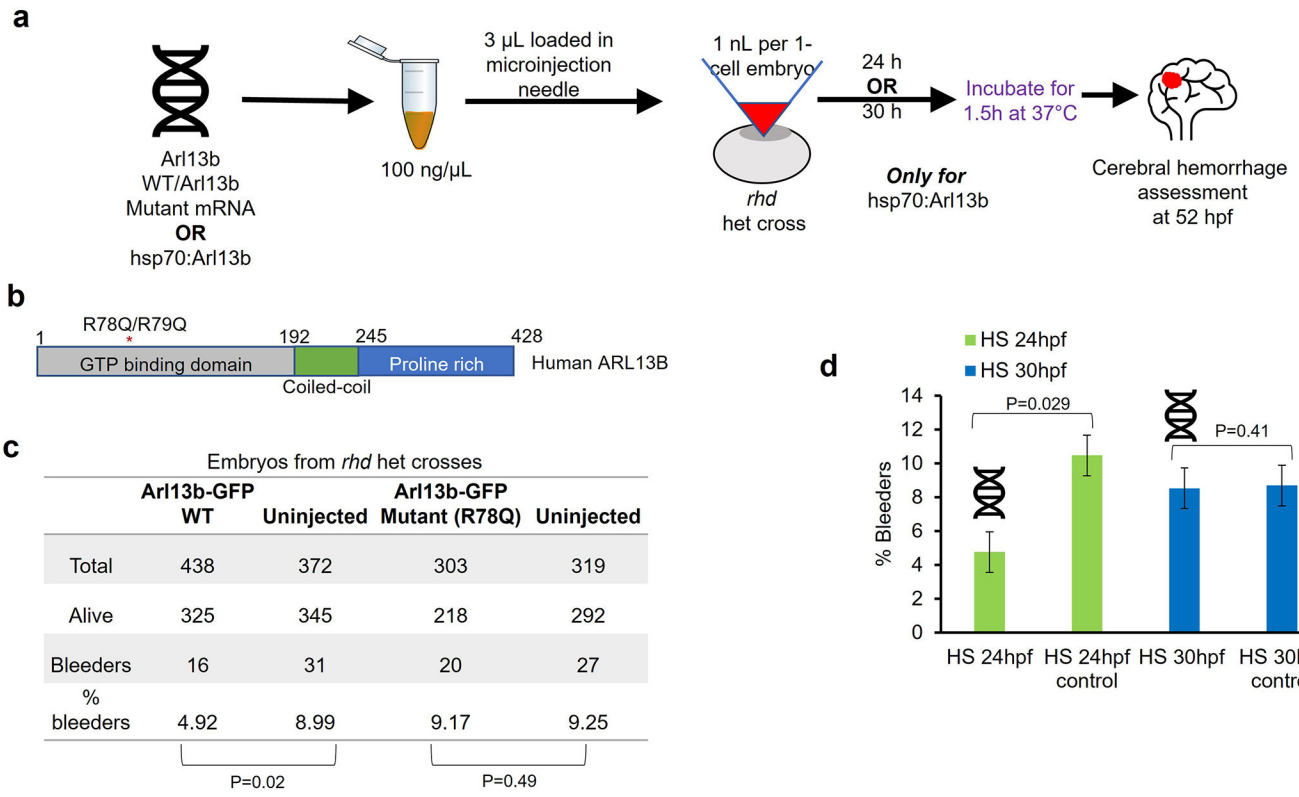

Figure 3. *Arl13b* WT not mutant mRNA expression is required at a specific time point for vascular stability *in vivo*.

a. This panel is a cartoon representation of the experimental design for approaches 2 and 3 in the *Arl13b* mRNA injection experiments. **b.** Th protein domains in human ARL13B protein and the site of the R78/R79Q mutation found in Joubert Syndrome are depicted pictorally. **c**. A table of the data from the approach 2 injection experiment performed in *rhd* mutants. This experiment is pooled from n=8 with 40-50 embryos per sample per experiment. P values across groups are depicted in the table. **d.** Control HS group was not injected, and HS experimental groups were injected with hsp70:Arl13b plasmid. Both control HS and HS experimental groups was heat shocked at the time indicated. P = 0.03 between control HS and HS experimental groups at 24 hpf (n= 4) and P = 0.41 between control HS and HS experimental groups at 30 hpf (n=3). Embryo numbers for each group from all experiments are - Control HS 24 hpf: 314, HS 24 hpf (experimental): 149, Control HS 30 hpf: 512, HS 30 hpf (experimental): 64. Proportion of bleeders were compared using one-sided two sample Z test or Fisher's exact test. P<0.05 was considered significant.

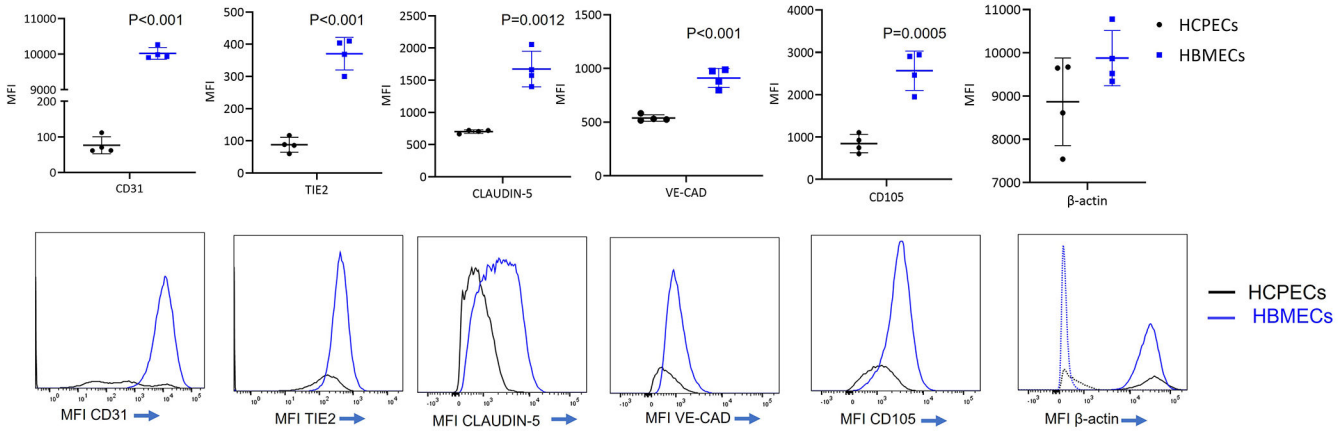

Figure 4. Validation of human primary brain microvascular ECs.

Human primary brain microvascular ECs were validated and compared with human primary brain choroid plexus endothelial cells for endothelial specific markers CD31, TIE2, Claudin-5, Ve-cadherin (VE-CAD), CD105 (endoglin) and β-actin by flow cytometry analysis (n=4). Expression of each protein is quantified as median fluorescence intensity (MFI). Results were presented as mean ± SEM. SEM, standard error to the mean. P<0.05 was considered significant. Top panel shows the quantification, while the bottom panel shows representative MFI histogram for respective proteins. For β-actin quantification, secondary antibody was used. Dotted histograms with respective colors mark 'secondary controls.'

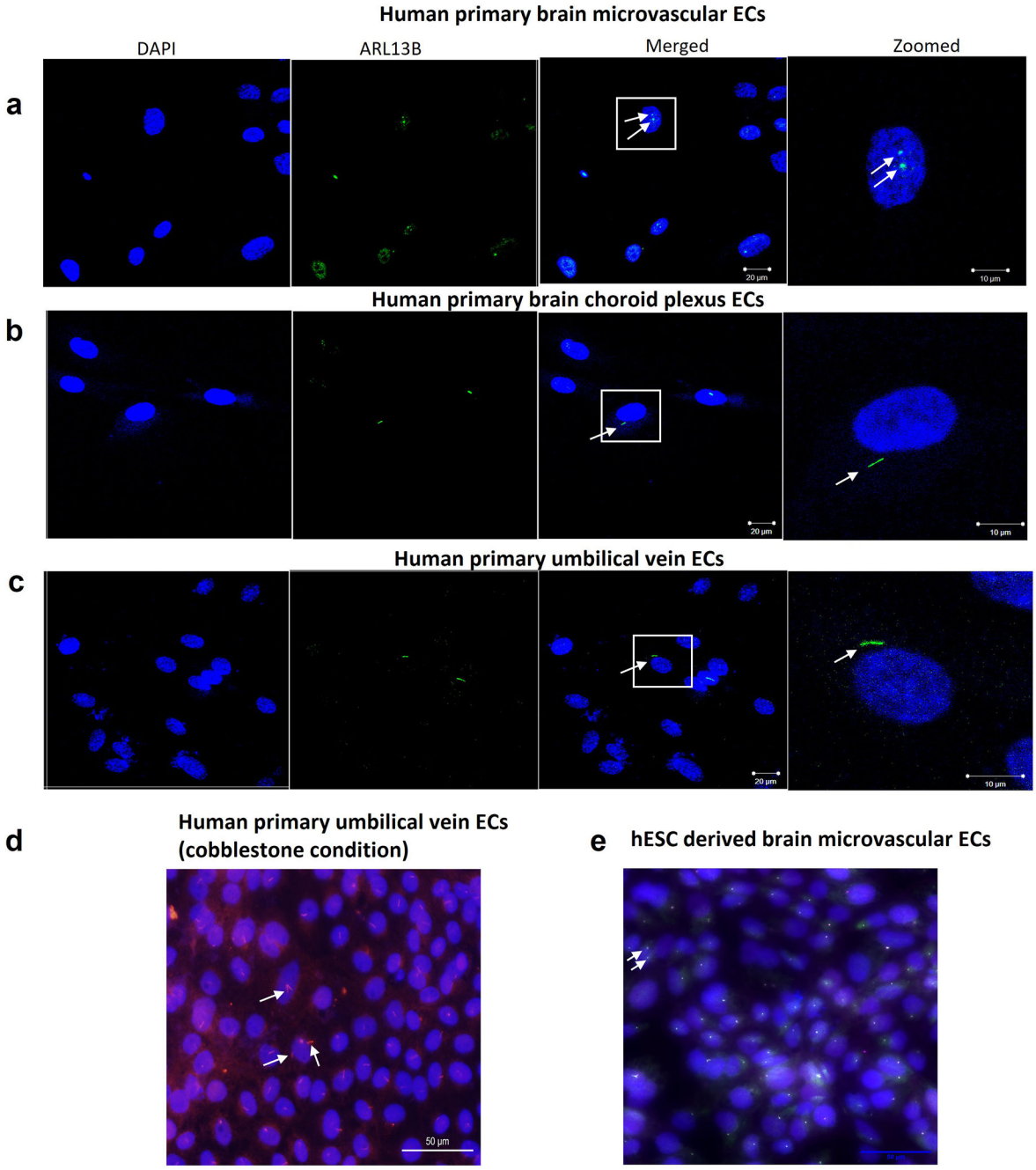

Figure 5. Comparison of cilia expression in multiple endothelial cell models.

a. Human primary brain microvascular ECs stained for ciliary protein ARL13B (green) and nuclear stain DAPI (blue) showing more than one cilia by immunofluorescence method. **b**. Human primary umbilical vein endothelial cells. **c**. Human primary brain choroid plexus endothelial cells. **a-c.** Scale bar are 20 µm in the merged image and 10 µm in the zoomed image (n=3). White boxed regions are zoomed in the adjacent panel and arrows indicate cilium. **d**. Human primary umbilical vein endothelial cells were grown for an additional 5 days once confluence was reached prior to cilia staining with acetylated tubulin (red)

antibody. Scale bar= 50 μm. Arrows show a cell with multiple cilia. **e**. Human embryonic stem cell-derived brain microvascular endothelial-like cells staining with ARL13B antibody. Scale bar= 50 μm. (n=4). Arrows show a cell with multiple cilia.

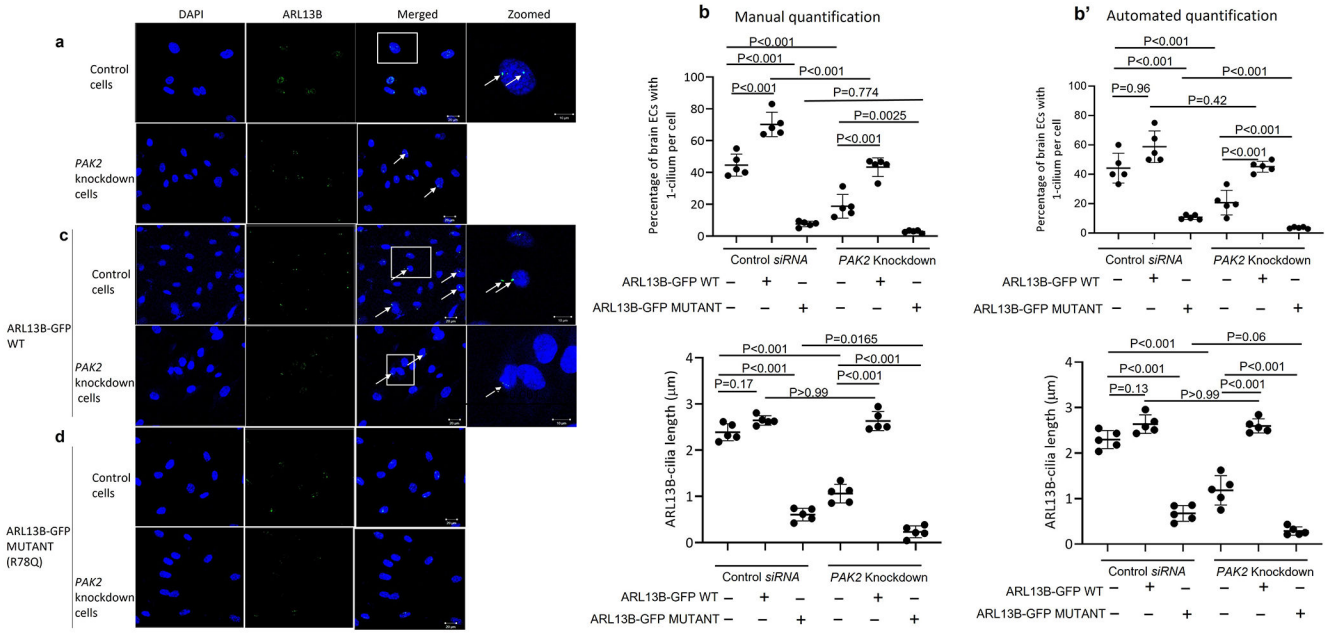

Figure 6. ***Arl13b*** **WT but not mutant rescues** ***PAK2*** **knockdown ciliogenesis in brain ECs.**

a, c & d. HBMECs were knocked down with and without *PAK2* siRNA (25 nM) (upper panel, **a**), with and without overexpression of *Arl13b-GFP WT* plasmid (middle panel, **c**), with and without overexpression of *Arl13b-GFP Mutant (R78Q)* plasmid (lower panel, **d**) and assessed for ARL13B positive cilia by immunofluorescence. Scale bar= 20 μm in the merged image and 10 μm in the zoomed image. **b.** Two graphs are depicted. The top graph represents percentage of brain ECs with 1 cilium per cell. Cells with 2-cilia were not included in the quantification. The bottom graph is the ARL13B cilia length measured in each sample set. Number of cilia and its length were assessed by number of nuclei to cilia and its length using ACDC V 0.93 cilia specific software. Each dot represents random field in the slide. Statistical P values were compared to control group; n=3 in each experimental group. Detailed quantification protocol is provided in the methods section. Results were presented as mean ± SEM. SEM, standard error to the mean. ANOVA was used to examine the effects of various conditions on the outcomes.

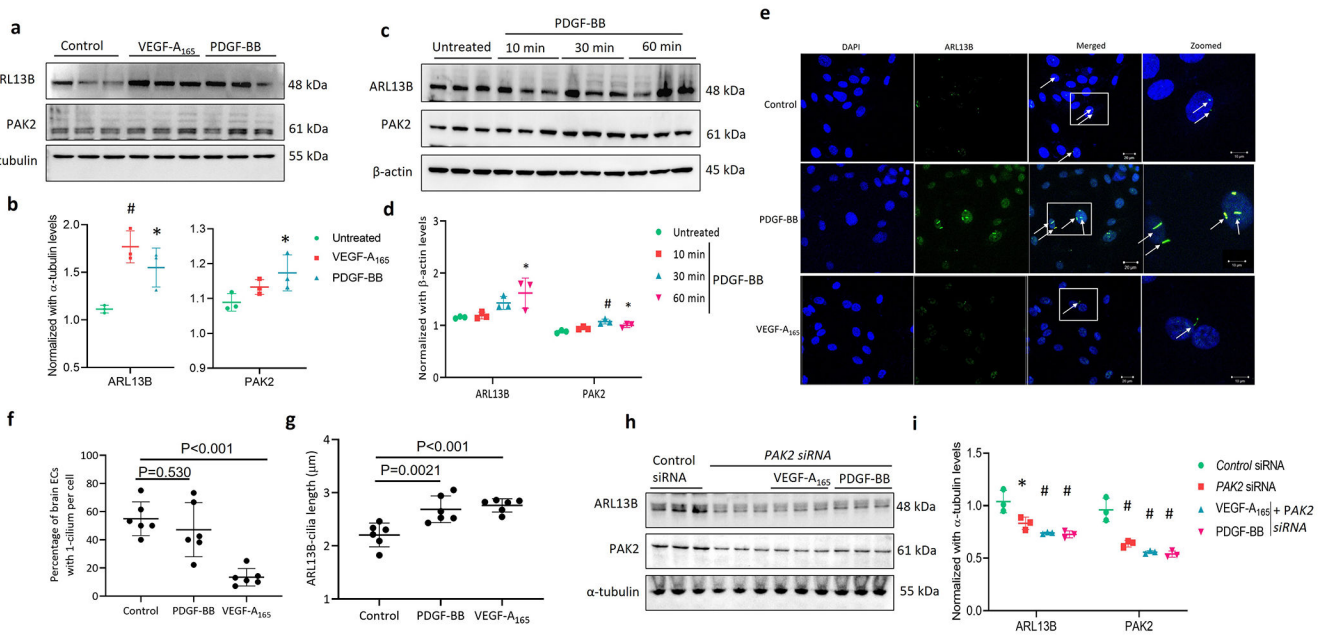

Figure 7. VEGF-A and PDGF-BB ligands induce ARL13B-PAK2-mediated ciliogenesis in brain ECs.

a & **b.** Human brain microvascular endothelial cells (HBMECs) were treated with VEGF-A_{165} (20 ng/mL) and PDGF-BB ligands (10 ng/mL) for 5 and 60 mins respectively and assessed by immunoblotting for ARL13B and PAK2 proteins and quantified. Panels **c** & **d** are HBMECs treated with PDGF-BB (10 ng/mL) ligand for 10, 30 and 60 mins and assessed for ciliary protein ARL13B and vascular stability protein PAK2 by immunoblotting and quantified. Experiment was done in triplicates and the results were presented as mean ± SEM. SEM, standard error to the mean. *P<0.05; and #P<0.001 compared with control group; n=3 in each experimental group. ANOVA was used to examine the effects of various conditions on the outcomes.

e-g. PDGF-BB and VEGF-A_{165} treated HBMECs were assessed for ARL13B positive cilia by immunofluorescence (**e**) and quantified (**f & g**). Number of cilia and its length were assessed by number of nuclei to cilia and its length using ACDC V0.93 cilia specific software. The percentage of brain ECs represents 1-cilium per cell. Cells with 2-cilia were excluded in this quantification. Control group n= 65 nuclei; PDGF-BB group n= 57 nuclei; VEGF-A_{165} group n= 72 nuclei. Results were presented as mean ± SEM. SEM. Scale bar= 20 μm in the merged image and 10 μm in the zoomed image. Each dot represents a random field in the slide. Statistical P values were compared to control group; n=3 in each experimental group. Detailed quantification protocol is provided in the methods section. **h** & **i.** HBMECs were knocked down with *PAK2* siRNA with and without the EC ligands VEGF-A_{165} and PDGF-BB for 5 and 60 mins and assessed for PAK2 and ARl13B levels by immunoblotting. (*P<0.05 and #P<0.001 compared with control group; n=3 in each experimental group). Results were presented as mean ± SEM. ANOVA was used to examine the effects of various conditions on the outcomes.

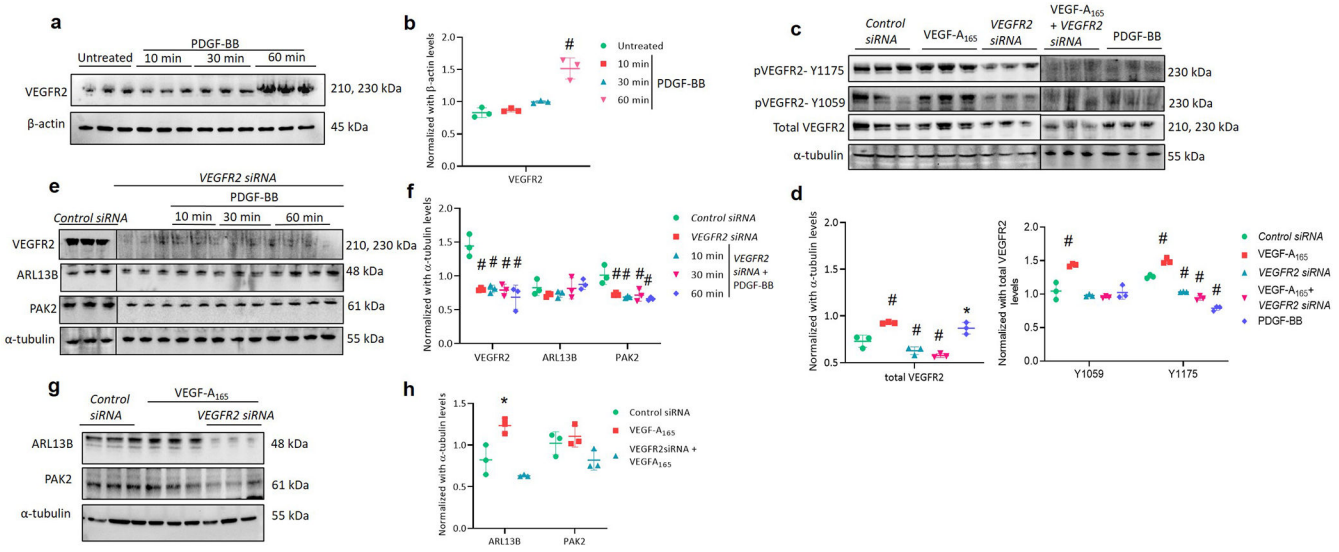

Figure 8. VEGFR2 is needed for VEGF-A and PDGF-BB-induced PAK2-ARL13B ciliogenesis in brain ECs.

a & **b**. Human brain microvascular endothelial cells (HBMECs) were treated with PDGF-BB (10 ng/mL) ligand for 10, 30 and 60 mins and assessed for total VEGFR2 protein levels and quantified. **c** & **d**. HBMECs were treated with VEGF-A_{165} for 5 mins, *VEGFR2* siRNA, VEGF-A_{165} + *VEGFR2* siRNA and PDGF-BB ligand for 60 mins and assessed for phosphorylated VEGFR2 at tyrosine sites Y1175 and Y1059 and total VEGFR2 protein levels and quantified. *P<0.05; **P<0.01 and #P<0.001 compared with control group; n=3 in each experimental group. Results were presented as mean ± SEM. **e** & **f.** HBMECs knockdown with *VEGFR2* siRNA (25 nM) and treated with PDGF-BB 10, 30 and 60 mins respectively and assessed for VEGFR2, ciliary protein ARL13B and vascular stability protein PAK2 and quantified. **g** & **h**. HBMECs treated with VEGF-A_{165} (20 ng/mL) and knockdown with *VEGFR2* siRNA respectively and assessed for ARL13B and PAK2 proteins and quantified. ANOVA was used to examine the effects of various conditions on the outcomes.